

The intermediate and spin-liquid phase of the half-filled honeycomb Hubbard model

Qiaoni Chen,¹ George H. Booth,¹ Sandeep Sharma,¹ Gerald Knizia,^{1,2} and Garnet Kin-Lic Chan^{1,3}

¹*Department of Chemistry, Princeton University, Princeton, NJ 08544*

²*Institut fuer Theoretische Chemie, Universitaet Stuttgart,
Pfaffenwaldring 55, D-70569 Stuttgart, Germany*

³*Department of Physics, Princeton University, Princeton, NJ 08544*

We obtain the phase-diagram of the half-filled honeycomb Hubbard model with density matrix embedding theory, to address recent controversy at intermediate couplings. We use clusters from 2-12 sites and lattices at the thermodynamic limit. We identify a paramagnetic insulating state, with possible hexagonal cluster order, competitive with the antiferromagnetic phase at intermediate coupling. However, its stability is strongly cluster and lattice size dependent, explaining controversies in earlier work. Our results support the paramagnetic insulator as being a metastable, rather than a true, intermediate phase, in the thermodynamic limit.

PACS numbers: 71.10.-w, 71.10.Fd, 71.30.+h, 75.10.Kt, 71.20.-b, 71.15.-m

Recently, there has been much debate over the zero-temperature phases of the Hubbard honeycomb model at half-filling. The accepted picture for many years was that for small interactions U , the system is semi-metallic (SM) with a Dirac cone in the density of states [1]; at large U , the system is antiferromagnetically long-range ordered (AFM) [2, 3]. However, Meng *et al.* proposed recently that an *additional* phase appears at intermediate couplings, arising from strong quantum fluctuations due to the low coordination number [4]. This phase has been further suggested to be a *gapped spin liquid* [5–8]. If present, this would be extremely significant, as spin liquids are not known to exist at half-filling without frustration [9–11], and would greatly advance the search for experimental realizations of 2D spin-liquids, both in correlated honeycomb materials as well as optical lattices [12, 13].

A large number of numerical methods have been applied to study the honeycomb Hubbard model [1–4, 11, 14–31]. The work by Meng *et al.* used zero-temperature auxiliary-field (determinant) quantum Monte Carlo (AFQMC) [4]. These results were viewed with particular confidence because AFQMC has no sign problem in this model and thus correlations were treated “exactly”, the only errors arising from using a finite size lattice of 648 sites. Subsequent to this, many reports of an intermediate phase have appeared using quantum cluster methods [32], such as Cluster Dynamical Mean-Field Theory (CDMFT) with exact diagonalization (ED) (Liebsch [24] and He *et al.* [26]) and quantum Monte Carlo (CT-QMC) solvers (Wu *et al.*) [28], and the Variational Cluster Approximation (VCA) [27]. While these various quantum cluster methods differ in some details, they share a unifying Green function and self-energy functional formulation [33, 34], thus we refer to them collectively as Green function cluster (GFC) methods.

Despite these initial reports, there now appears increasing evidence that there may in fact be no spin-liquid phase [11, 18, 20]! The strongest hint is from Sorella *et*

al. [20], who repeated Meng’s AFQMC calculation with a larger lattice of 2592 sites. They found that at the increased lattice size, the region for an intermediate phase shrank significantly, suggesting weak (if any) evidence for a spin-liquid phase. Subsequently, a further VCA calculation by Hassan and Senechal, in contrast to earlier quantum cluster calculations, also found no spin-liquid phase [11].

These conflicting reports raise important questions both for the physics of the honeycomb Hubbard model, and the numerical methods used to study it. Is there an intermediate phase, and is it a spin-liquid? If not, what is observed in calculations which see an intermediate phase - is the system “close” to a spin-liquid or some other state? Why do some quantum cluster calculations observe an intermediate phase and others not? And how do the various numerical approximations, such as finite lattice size in AFQMC, or finite cluster size in GFC methods, bias the calculations? These are the main questions we target in this work.

To answer these questions, we use a different quantum cluster method to those used previously - the recently proposed Density Matrix Embedding Theory (DMET) [35–38]. Note that DMET is not a variant of the GFC methods discussed above. In principle, GFC methods complement AFQMC, because they work in the thermodynamic limit, but only treat a finite range of correlations determined by the impurity cluster size. In practice, however, solving the impurity problem within GFC methods involves further numerical approximations, such as bath discretization, or analytic continuation. Both require careful treatment to avoid affecting the physics. In contrast, DMET is a quantum cluster method without bath discretization error by construction, and which yields a quantum impurity problem where spectral functions can be practically computed without analytic continuation. This allows us to study the honeycomb Hubbard model as a function of cluster correlation length and at the thermodynamic limit with no further extraneous

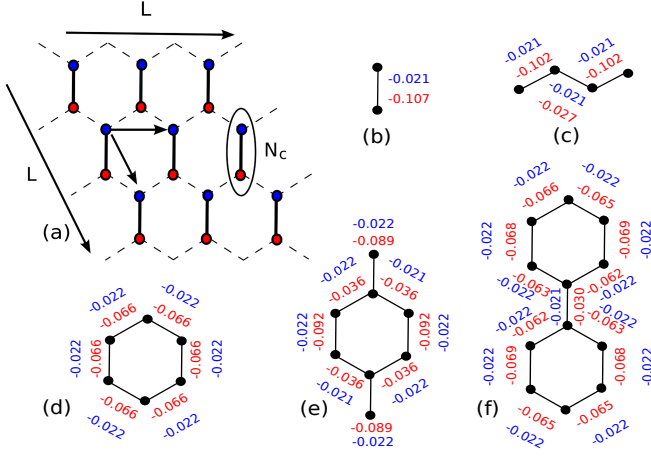


FIG. 1. (Color online) (a) DMET embeds clusters of N_c sites in the underlying honeycomb lattice of $2L^2$ sites. (b)–(f) Cluster shapes in our study, for $N_c = 2 - 12$. Also shown is the nearest-neighbour spin-spin correlation, $\langle S_i^z S_j^z \rangle$. Blue numbers are from $U = 1.5t$ in the semi-metal (SM) phase, red numbers from $U = 8.4t$ in the paramagnetic insulator (PMI) phase.

numerical approximations.

DMET maps a large lattice problem to a quantum impurity plus bath problem, and is exact in the weak- and strong-coupling limits, as well as the limit of infinite cluster size. The main conceptual difference between DMET and GFC methods [39–42], is that the DMET bath is derived from the *entanglement* of the quantum state of the impurity cluster, rather than its single-particle Green function. DMET has several important technical advantages. If one is interested in thermodynamic properties, no Green functions need be computed; only the ground-state quantum impurity problem is solved, a significant computational savings. Further, since the DMET bath is defined from a Schmidt decomposition, the bath is *the same size as the impurity with no bath discretization error*, in contrast to the infinite bath in DMFT. Typically, an n -site cluster ($n > 1$) DMET calculations yields similar physics to an n -site CDMFT that is converged with respect to the bath parametrization, even though the DMET calculations require only a fraction of the cost [35–38].

We now describe the DMET method briefly; for more details we refer to the original references [35–37]. We first choose an impurity cluster, cut from the underlying lattice. The underlying lattice is finite, but can trivially be made very large: in this study, we use lattices with more than 90,000 sites. The “environment” lattice sites outside the cluster are then replaced by a bath. In ground-state DMET, the bath is defined with the help of a model lattice ground-state wavefunction $|\Psi^{(0)}\rangle$. In this study, $|\Psi^{(0)}\rangle$ is a (possibly spin-broken) Slater determinant (ground-state) of a non-interacting lattice Hamiltonian $h + u$, where h is the hopping matrix, and u is

a frequency-independent one-particle operator acting in each cluster cell on the lattice, analogous to a cluster self-energy. For ground-state DMET, the Schmidt decomposition of $|\Psi^{(0)}\rangle$ between the cluster and environment defines a bath space $\{|\beta^0\rangle\}$, of the same size as the impurity space. The quantum impurity Hamiltonian H' is then obtained by projecting a model lattice Hamiltonian H_{lat} onto the quantum impurity plus bath space,

$$\begin{aligned} H' &= PH_{lat}P \\ &= P(h + U_{cluster} + u)P \end{aligned} \quad (1)$$

where $U_{cluster}$ indicates that in H_{lat} , Hubbard interactions are present only on the cluster sites, as in CDMFT, while the one-particle operator u is used for lattice sites outside the cluster, i.e. there are no interactions in the bath. Solving for the ground-state of H' is a many-body problem with twice the degrees of freedom as the impurity cluster. The resulting quantum impurity wavefunction yields expectation values, such as energies and correlation functions that approximate those of the original lattice problem. u is adjusted to minimize the difference between the single-particle density matrix $\langle a_i^\dagger a_j \rangle$ of H' and the ground-state of the model lattice Hamiltonian $h + u$ projected to the impurity plus bath space, analogous to the self-consistent update of the self-energy in DMFT.

To obtain spectra in DMET a modified procedure is used, where the ground-state bath space $\{|\beta^0\rangle\}$ is augmented to reproduce dynamical properties. For example, to compute the local single-particle Green function, we consider the response vector of the model lattice wavefunction,

$$|\Psi^{(1)}(\omega)\rangle = \frac{1}{\omega + \mu - h + u + i0} a_\alpha^\dagger |\Psi^{(0)}\rangle \quad (2)$$

and obtain a set of *additional* bath states from the Schmidt decomposition of $|\Psi^{(1)}(\omega)\rangle$, leading to a total bath space $\{|\beta^0\rangle \oplus |\beta^1(\omega)\rangle\}$. The cluster Green function is determined by solving, at each frequency, the response problem for H_{lat} projected into the impurity plus dynamical bath space. Although the bath space is finite, it changes with frequency, thus the finite impurity model produces a *continuous* spectrum along the real axis without artificial broadening.

We now turn to applying DMET to the honeycomb Hubbard model. To identify different phases we monitor several quantities. The SM phase is characterized by a vanishing single-particle gap and a Dirac cone at low energies in the single-particle density of states $A(\omega)$. The AFM phase is characterized by non-vanishing staggered magnetization, $M = \frac{1}{N} \sum_{ij} (-1)^{i+j} (n_{i\uparrow} - n_{j\downarrow})$, a non-zero single-particle gap (which grows with increasing U), and a vanishing spin-gap. The proposed intermediate gapped phase is identified by a non-vanishing single-particle and spin-gap without long-range AFM order. We

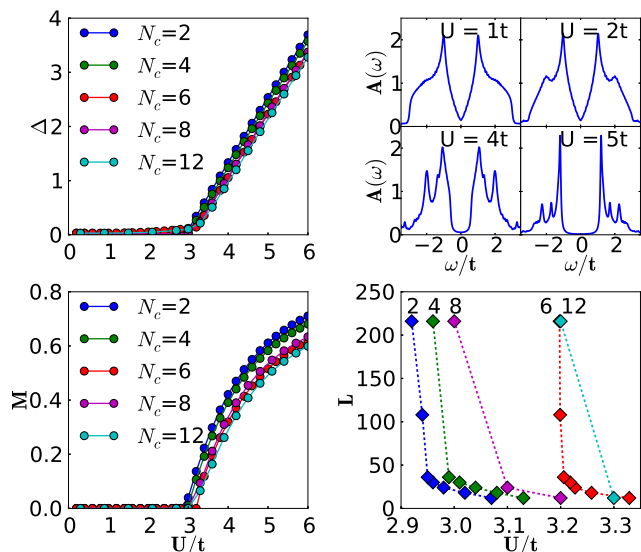


FIG. 2. (Color online) DMET calculations allowing spontaneous AFM order. Top Left: Single-particle gap against U for cluster sizes $N_c = 2 - 12$. As U increases, a gap spontaneously opens at U_{AFM1} , just after $U = 3$. Top Right: Local density of states when $N_c = 6$, calculated from spectral DMET [37], showing the Dirac cone in the SM phase. Bottom Left: Staggered magnetization against U for $N_c = 2 - 12$. The staggered magnetization appears at the same point as the opening of the gap. Bottom Right: U_{AFM1} as a function of lattice size $L = 12 - 216$ (288 – 93312 sites) and cluster size ($N_c = 2 - 12$).

further check for spin-liquid character from the correlation functions. Meng *et al.* [4] further suggested that the intermediate phase can be identified from the gradient of dT/dU , where T is the kinetic energy. Not all the above quantities have been of equal focus in earlier studies; AFQMC studies report energies and gaps but not spectral functions, while GFC calculations report spectral quantities but not energies. Here, using DMET, we study energies as well as gaps and spectral functions.

To study the effect of cluster size and shape, we perform calculations with $N_c = 2 - 12$ cluster sites; these are shown in Fig. 1. For $N_c = 2 - 6$ (4 – 12 sites with the bath) we use an exact diagonalization solver; for $N_c = 8 - 12$ (16 – 24 sites with bath) we use a density matrix renormalization group (DMRG) solver [43], keeping up to 2000 states, sufficient for quasi-exactness. It is important to distinguish cluster size N_c from the size of the lattice ($2L^2$) in which the cluster is embedded. To study finite-size scaling effects of the underlying lattice, we use embedding lattices with $L \times L$ supercells ($2L^2$ sites), with $L = 12 - 216$ (up to over 90,000 sites). The smaller L calculations allow direct comparison to finite AFQMC calculations: for comparison, Meng *et al.* used up to $L = 18$; Sorella *et al.* used up to $L = 36$.

We start by scanning the phase diagram as a func-

tion of U , allowing spontaneous antiferromagnetism to develop. The single-particle gap, magnetization, and density of states for $N_c = 2 - 12$ are shown in Fig. 2. We see at small U the single particle gap vanishes and the density of states displays a low-energy Dirac cone, clearly demonstrating that the system is in the SM phase. As we increase U beyond a critical U_{AFM1} an AFM solution to the DMET equations appears and a gap opens in the spectral function (Fig. 2). Note that U_{AFM1} is the earliest point at which the AFM solution can be found but this does not indicate a thermodynamic phase transition at this point, which requires a more detailed examination of the energies, discussed below. At U_{AFM1} , the single-particle gap and magnetization vanish simultaneously. Fitting $M = |U - U_{\text{AFM1}}|^\beta$ to the $N_c = 6$ data gives a critical exponent $\beta = 0.72$, compared with 0.80 ± 0.04 from the AFQMC calculations of Sorella *et al.*, and $\beta = 1$ from mean-field. U_{AFM1} shows significant cluster and lattice size dependence, as seen in Fig. 2; for $N_c = 6$, $L = 12 - 216$, U_{AFM1} decreases from 3.329 to 3.198, while at $L = 216$, for $N_c = 2 - 12$, U_{AFM1} increases from 2.92 to 3.2. Our $U_{\text{AFM1}} = 3.2$ for $N_c = 12$, $L = 216$ is somewhat lower than the recent AFQMC result $U_{\text{AFM1}} = 3.869$ of Sorella *et al.* [20]. The lattice size dependence of U_{AFM1} gives an estimate of the finite size error in Sorella *et al.*'s $L = 36$ calculations; from $L = 36 - 216$, U_{AFM1} decreases by ~ 0.01 .

A quantitative check of the accuracy of our calculations is to directly compare the energies for a given finite size lattice with the exact AFQMC energies for the same lattice size. This comparison for total energies is shown in Fig. 4. We have compared over only a limited range of U as this is where we had access to the QMC data [20]. However, theoretically and numerically it is known that the error in the DMET energies vanishes exactly at weak and strong coupling; the largest errors are near phase transitions [35], the region tested in Fig. 4. Even in this challenging region, the cluster DMET total energies appear extremely good, as expected from earlier benchmarks [35, 36, 38]; with $N_c = 12$ the energies are within 0.2% of the exact results. The more sensitive kinetic-energy derivative dT/dU reported by Meng *et al.* (and obtained from Sorella *et al.*) is also shown in Fig. 5. Here we find that although Meng *et al.* argued that the two changes in curvature in dT/dU near $U = 3.5, 4.3$ indicate an intermediate phase, we also observe two changes in curvature in our cluster DMET curve, at similar places, with just a SM and AFM phase, showing this is not a good diagnostic for an intermediate phase.

We now consider the intermediate U region and look for evidence of possible *metastable* intermediate phases. To do so, we restrict our DMET calculations to paramagnetic phases and increase U . Interestingly, as U is increased, we observe two kinds of paramagnetic transitions depending on cluster shape: for $N_c = 2, 4, 8$ there is a first-order transition to a gapped phase, while for

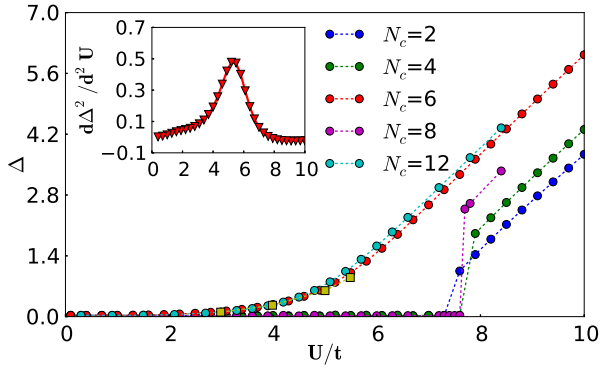


FIG. 3. (Color online) Single particle gap of paramagnetic solution with cluster sizes for $L = 216$. For $N_c = 2, 4, 8$ the transition is first order; for $N_c = 6, 12$ the transition is continuous. Inset: second derivative of the gap for $N_c = 6, 12$; we identify U_{PM} from the peak. Yellow squares: 6-site CDMFT calculations from Ref. [1].

$N_c = 6, 12$, there is a second-order transition: the gap opens continuously. In either case, we find a paramagnetic insulating phase (PMI) at large U . This finding of a PMI phase is not unexpected; preceding 6-site GFC calculations have identified a similar phase, typically identified as a Mott insulator. We can compare the $N_c = 6$ DMET PMI gaps directly to earlier 6-site paramagnetic GFC calculations (see [1] for a summary). The agreement at large U is good, but DMET does not produce the spurious gap seen in some GFC calculations at small U that has led to erroneous conclusions that there is no SM phase [11]. Note further, that we find the paramagnetic transition U_{PM} is very sensitive to cluster size, as seen in Fig. 3.

Hassan and Senechal conjectured that the purported spin-liquid phase in the honeycomb Hubbard model *is* in fact the PMI phase in a quantum cluster calculation [11]. We now examine this conjecture. To identify whether the PMI phase is a true intermediate phase, we must check its stability in the presence of antiferromagnetism. In the square lattice, antiferromagnetism order appears at infinitesimal U before the PMI phase is reached. The honeycomb Hubbard model differs in this regard because AFM order develops at finite U_{AFM1} , which could in principle be larger than U_{PM} . In Fig. 5 we show the energy of the AFM phase relative to the SM/PMI phases as a function of cluster and lattice size. Here, we find that for our cluster sizes the transition between SM and AFM does *not* in fact occur at U_{AFM1} , rather there is a first-order coexistence region between U_{AFM1} , U_{AFM2} , where U_{AFM2} is strongly cluster size (and to a lesser degree lattice size) dependent (Fig. 5). As the cluster size increases, the first-order coexistence region decreases, and it appears that in the limit of infinite cluster size the true AFM transition is second-order (Fig. 5). Further, in all instances we have studied, $U_{\text{AFM2}} < U_{\text{PMI}}$ at the same

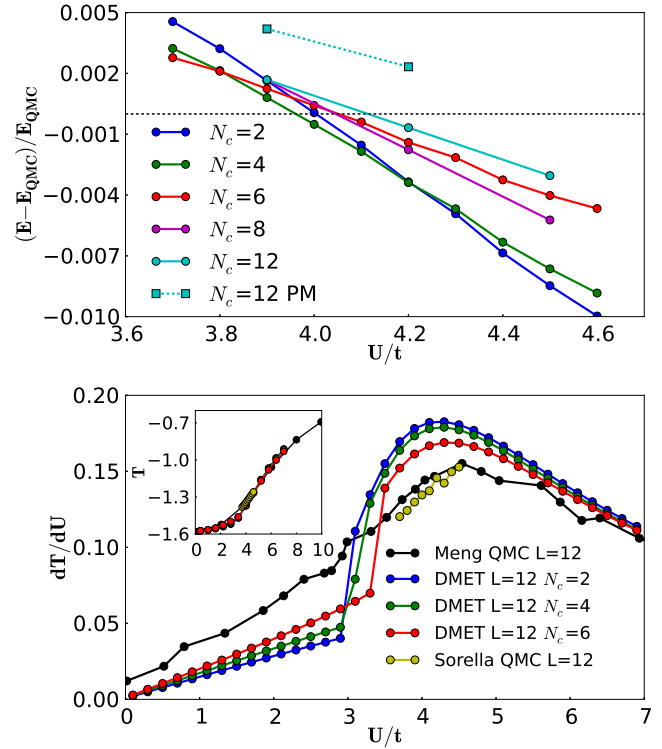


FIG. 4. (Color online) Top: DMET energy versus Sorella *et al.*'s finite lattice AFQMC energy at intermediate U for $L = 12$ (288 sites) as a function of cluster size $N_c = 2 - 12$. This is the most challenging regime for DMET, but the energy comparison is very favourable. PM denotes paramagnetic solution. Bottom: Derivative of kinetic energy as a function of U/t . Overlaid are results of Meng *et al.* and Sorella *et al.* for $L = 12$ [4]. Inset: Kinetic energy density as a function of U , showing good agreement between the DMET and numerically exact AFQMC [4]. DMET qualitatively reproduces two changes in curvature (near $U = 3.5$ and $U = 4.3$) cited as evidence of an intermediate phase by Meng *et al.*, although no intermediate phase is observed.

cluster size. This means that there is in fact *no* stable intermediate paramagnetic phase. However, for the special cluster sizes $N_c = 6, 12$, the PMI phase is particularly competitive, and for these clusters, U_{AFM2} is very close to U_{PM} . Since locating U_{PM} precisely is itself difficult due to its continuous nature, a small uncertainty in U_{PM} could then yield $U_{\text{PM}} < U_{\text{AFM2}}$, and a conclusion that there is a true paramagnetic intermediate phase. In addition, the very small difference between U_{AFM2} and U_{PM} provides a basis to explain the conflicting observations, in both AFQMC and in GFC calculations, of an intermediate phase near the antiferromagnetic transition: small changes in calculation parameters can selectively stabilize the PMI phase. Our arguments therefore support the interpretation of Hassan *et al.* that observations of the “intermediate” phase can be identified with the PMI state in quantum cluster calculations.

What is the nature of the metastable paramagnetic

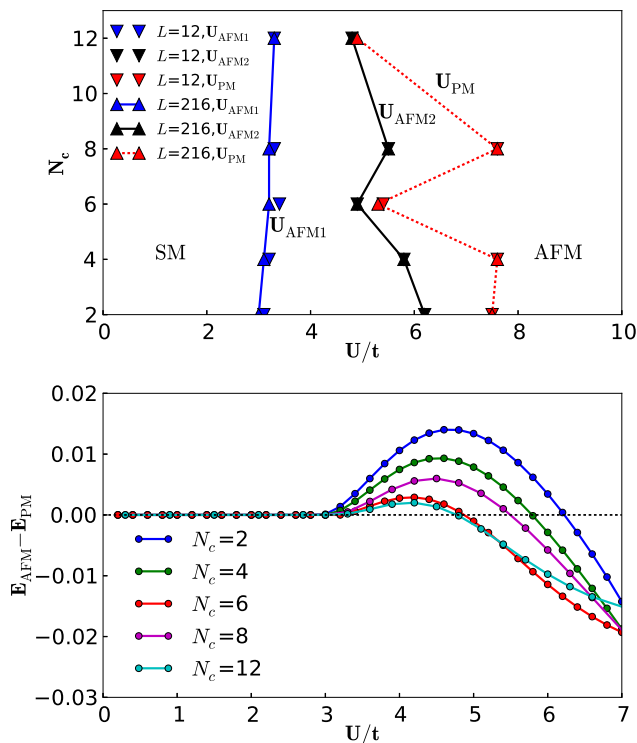


FIG. 5. (Color online) Top: Phase transition points as a function of cluster size 2-12, and two lattice sizes $L = 12, 216$. U_{AFM1} corresponds to opening of the gap. U_{AFM2} corresponds to the thermodynamic transition to the AFM phase. $[U_{AFM1}, U_{AFM2}]$ is a coexistence region for the AFM phase and SM phase, although this region appears to vanish with increasing cluster size. U_{PM} is the transition to the PMI if AFM order is not allowed to develop. The transition is first order for $N_c = 2, 4, 8$ and second order for $N_c = 6, 12$. Note that for $N_c = 6, 12$, U_{PM} is very close to U_{AFM2} indicating that the PMI is very competitive with the AFM phase for these cluster shapes. Bottom: Ground state energy difference of PM and AFM solutions. The positive region is the coexistence region.

state for $N_c = 6, 12$? Although this “intermediate phase” is gapped without long-range magnetic order, this does not mean that it is a spin-liquid; another obvious candidate would be some kind of valence-bond crystal. The particular stabilization of the paramagnetic insulator for the hexagonal based clusters $N_c = 6, 12$, suggests that it is associated with a hexagonal cluster (valence-bond crystal) order. The annotations in Fig. 1 show the spin-spin correlation functions $\langle S_i^z S_j^z \rangle$. Although these correlation functions in cluster DMET (as in CDMFT) are not guaranteed to preserve translational invariance, the pattern of translational invariance breaking can be revealing of an underlying order. Indeed, the spin-correlation functions for $N_c = 12$ confirm that a hexagonal cluster order develops in this PMI phase (note there is no symmetry breaking in the corresponding SM phase for $N_c = 12$, and further that the single $N_c = 6$ cluster shows no ev-

idence of dimerization). Intriguingly, hexagonal cluster order has been implicated as a real instability of graphene under strain [44]. The (uncompetitive) PMI phase for $N_c = 2, 4, 8$ develops a simpler dimer order.

In conclusion, we have carried out cluster DMET calculations, as a function of cluster and lattice size, to elucidate the phase-diagram of the half-filled Hubbard honeycomb model. Our detailed calculations find that at intermediate couplings, there is a metastable paramagnetic insulating phase, that is very competitive with the antiferromagnetic phase. This insulating phase displays an associated hexagonal cluster order. The closeness of the two phases at intermediate couplings means that small changes in calculational details can significantly affect their relative stability, and this explains the large number of conflicting results regarding the intermediate phase. It further seems likely that the intermediate paramagnetic phase can be stabilized by introducing modest frustration. Finally our work demonstrates the potential of the DMET methodology, which allows computation of both energies and spectral functions at the thermodynamic limit, without incurring additional numerical artifacts.

We gratefully acknowledge S. Sorella and Y. Otsuka for providing the energy data from their QMC calculations. This work was funded by the US Department of Energy, primarily through DE-SC0008624 and DE-SC0010530. Additional funding was provided through the DOE-CMCSN program DE-SC0006613.

-
- [1] A. Liebsch and W. Wu, Phys. Rev. B **87**, 205127 (2013).
 - [2] S. Sorella and E. Tosatti, Europhys. Lett. **19**, 699 (1992).
 - [3] L. Martelo, M. Dzierzawa, L. Siffert, and D. Baeriswyl, Z. Phys. B **103**, 335 (1997).
 - [4] Z. Y. Meng, T. C. Lang, S. Wessel, F. F. Assaad, and A. Muramatsu, Nature **464**, 847 (2010).
 - [5] F. Wang, Phys. Rev. B **82**, 024419 (2010).
 - [6] C. Xu, Phys. Rev. B **83**, 024408 (2011).
 - [7] Y.-M. Lu and Y. Ran, Phys. Rev. B **84**, 024420 (2011).
 - [8] B. K. Clark, ArXiv e-prints **1305**, 0278 (2013), arXiv:1305.0278 [cond-mat.str-el].
 - [9] L. Balents, Nature **464**, 199 (2010).
 - [10] I. Kimchi, S. A. Parameswaran, A. M. Turner, F. Wang, and A. Vishwanath, Proc. Nat. Acad. Sci. U.S.A. **110**, 16378 (2013).
 - [11] S. R. Hassan and D. Sénéchal, Phys. Rev. Lett. **110**, 096402 (2013).
 - [12] K. S. Novoselov, A. K. Geim, S. V. Morozov, D. Jiang, Y. Zhang, S. V. Dubonos, I. V. Grigorieva, and A. A. Firsov, Science **306**, 666 (2004).
 - [13] R. Walters, G. Cotugno, T. H. Johnson, S. R. Clark, and D. Jaksch, Phys. Rev. A **87**, 043613 (2013).
 - [14] J. E. Drut and T. A. Lähde, Phys. Rev. Lett. **102**, 026802 (2009).
 - [15] J. E. Drut and T. A. Lähde, Phys. Rev. B **79**, 165425 (2009).
 - [16] T. Paiva, R. T. Scalettar, W. Zheng, R. R. P. Singh, and

- J. Oitmaa, Phys. Rev. B **72**, 085123 (2005).
- [17] K. L. Lee, K. Bouadim, G. G. Batrouni, F. Hébert, R. T. Scalettar, C. Miniatura, and B. Grémaud, Phys. Rev. B **80**, 245118 (2009).
 - [18] B. K. Clark, D. A. Abanin, and S. L. Sondhi, Phys. Rev. Lett. **107**, 087204 (2011).
 - [19] H.-Y. Yang, A. Albuquerque, S. Capponi, A. M. Luchli, and K. P. Schmidt, New J. Phys. **14**, 115027 (2012).
 - [20] S. Sorella, Y. Otsuka, and S. Yunoki, Sci. Rep. **2**, 992 (2012).
 - [21] M.-T. Tran and K. Kuroki, Phys. Rev. B **79**, 125125 (2009).
 - [22] S. A. Jafari, Eur. Phys. J. B **68**, 537 (2009).
 - [23] W. Wu, Y.-H. Chen, H.-S. Tao, N.-H. Tong, and W.-M. Liu, Phys. Rev. B **82**, 245102 (2010).
 - [24] A. Liebsch, Phys. Rev. B **83**, 035113 (2011).
 - [25] K. Seki and Y. Ohta, arXiv:1209.2101 [cond-mat.str-el].
 - [26] R.-Q. He and Z.-Y. Lu, Phys. Rev. B **86**, 045105 (2012).
 - [27] S.-L. Yu, X. C. Xie, and J.-X. Li, Phys. Rev. Lett. **107**, 010401 (2011).
 - [28] W. Wu, S. Rachel, W.-M. Liu, and K. Le Hur, Phys. Rev. B **85**, 205102 (2012).
 - [29] T. Li, Europhys. Lett. **93**, 37007 (2011).
 - [30] A. Giuliani and V. Mastropietro, Commun. Math. Phys. **293**, 301 (2010).
 - [31] F. F. Assaad and I. F. Herbut, Phys. Rev. X **3**, 031010 (2013).
 - [32] T. Maier, M. Jarrell, T. Pruschke, and M. H. Hettler, Rev. Mod. Phys. **77**, 1027 (2005).
 - [33] M. Potthoff, Eur. Phys. J. B **32**, 429 (2003).
 - [34] M. Potthoff, Eur. Phys. J. B **36**, 335 (2003).
 - [35] G. Knizia and G. K.-L. Chan, Phys. Rev. Lett. **109**, 186404 (2012).
 - [36] G. Knizia and G. K.-L. Chan, J. Chem. Theory Comput. **9**, 1428 (2013).
 - [37] G. H. Booth and G. Kin-Lic Chan, arXiv:1309.2320 [cond-mat.str-el].
 - [38] D. J. Bulik I. W., Scuseria G. W., arXiv:1310.0051 [cond-mat.str-el].
 - [39] W. Metzner and D. Vollhardt, Phys. Rev. Lett. **62**, 324 (1989).
 - [40] A. Georges and W. Krauth, Phys. Rev. Lett. **69**, 1240 (1992).
 - [41] G. Kotliar, S. Y. Savrasov, K. Haule, V. S. Oudovenko, O. Parcollet, and C. A. Marianetti, Rev. Mod. Phys. **78**, 865 (2006).
 - [42] A. Georges, G. Kotliar, W. Krauth, and M. J. Rozenberg, Rev. Mod. Phys. **68**, 13 (1996).
 - [43] S. Sharma and G. K.-L. Chan, J. Chem. Phys. **136**, 124121 (2012).
 - [44] C. A. Marianetti and H. G. Yevick, Phys. Rev. Lett. **105**, 245502 (2010).